NeuroImage 222 (2020) 117257

Contents lists available at ScienceDirect

NeuroImage

journal homepage: www.elsevier.com/locate/neuroimage

Hierarchical cortical gradients in somatosensory processing

Noam Saadon-Grosman [a,*], Shahar Arzy [a,b,1], Yonatan Loewenstein [c,d,e,f,1]

[a] Department of Medical Neurobiology, Faculty of Medicine, The Hebrew University, 9112001 Jerusalem, Israel
[b] Department of Neurology, Hadassah Hebrew University Medical School, Jerusalem 9112001, Israel
[c] The Edmond and Lily Safra Center for Brain Sciences, The Hebrew University, 919040 Jerusalem, Israel
[d] The Alexander Silberman Institute of Life Sciences, The Hebrew University, 919040 Jerusalem, Israel
[e] Department of Cognitive Sciences, The Hebrew University, 919040 Jerusalem, Israel
[f] The Federmann Center for the Study of Rationality, The Hebrew University, 919040 Jerusalem, Israel

ARTICLE INFO

Keywords:
Stream
Large-scale organization
Selectivity
Laterality

ABSTRACT

Sensory information is processed in the visual cortex in distinct streams of different anatomical and functional properties. A comparable organizational principle has also been proposed to underlie auditory processing. This raises the question of whether a similar principle characterize the somatosensory domain. One property of a cortical stream is a hierarchical organization of the neuronal response properties along an anatomically distinct pathway. Indeed, several hierarchies between specific somatosensory cortical regions have been identified, primarily using electrophysiology, in non-human primates. However, it has been unclear how these local hierarchies are organized throughout the cortex. Here we used phase-encoded bilateral full-body light touch stimulation in healthy humans under functional MRI to study the large-scale organization of hierarchies in the somatosensory domain. We quantified two measures of hierarchy of BOLD responses, selectivity and laterality. We measured how selectivity and laterality change as we move away from the central sulcus within four gross anatomically-distinct regions. We found that both selectivity and laterality decrease in three directions: *parietal*, posteriorly along the parietal lobe, *frontal*, anteriorly along the frontal lobe and *medial*, inferiorly-anteriorly along the medial wall. The decline of selectivity and laterality along these directions provides evidence for hierarchical gradients. In view of the anatomical segregation of these three directions, the multiplicity of body representations in each region and the hierarchical gradients in our findings, we propose that as in the visual and auditory domains, these directions are streams of somatosensory information processing.

1. Introduction

1.1. Processing streams in the cortex

A central theme in neuroscience is that visual information is processed in the cortex in (at least) two distinct pathways, known as the dorsal and the ventral streams (Huang and Sereno, 2018; Kravitz et al., 2011; Milner and Goodale, 2006). Both streams originate in the primary visual cortex: the dorsal stream stretches to the parietal lobe whereas the ventral stream terminates in the inferior temporal lobe (Goodale and Milner, 1992; Huang and Sereno, 2018; Kravitz et al., 2011; Ungerleider and Mishkin, 1982). Several lines of evidence support this streams' hypothesis: (1) there is functional dissociation between the two streams. To a first approximation, the dorsal stream is oriented towards "where" processing whereas the ventral towards "what" processing (Ungerleider and Mishkin, 1982; Binkofski and Buxbaum, 2013; Kravitz et al., 2011). (2) Multiple visual field maps are present in different cortical areas (DeYoe and Van Essen, 1988; Grill-Spector and Malach, 2004; Wandell et al., 2007; Wandell and Winawer, 2011). (3) Many experiments provide evidence for hierarchical processing. First, electrophysiological measurements of response latencies demonstrate that visual information is sequentially processed along the streams (Arroyo et al., 1997; Culham, 1998; Martin et al., 2019; Schmolesky et al., 1998; Takaura et al., 2016). Second, the receptive fields of neurons increase in size and complexity along the processing streams (e.g., Burkhalter and Van Essen, 1986; Kastner et al., 2001; Rousselet et al., 2004; Yoshor et al., 2007). Finally, there is some evidence that neural responses become more bilateral along the stream (respond to both hemifields) (Pigarev et al., 2001). While preliminary evidence in support of hierarchical processing came from single neuron recordings, population receptive field (pRF) was used to measure the progressive increase in receptive fields away from the primary

* Corresponding author.
E-mail address: noam.saadongros@mail.huji.ac.il (N. Saadon-Grosman).
[1] These authors contributed equally to this work.

https://doi.org/10.1016/j.neuroimage.2020.117257
Received 24 November 2019; Received in revised form 6 August 2020; Accepted 7 August 2020
Available online 18 August 2020

visual cortex (Amano et al., 2009; Dumoulin and Wandell, 2008). Most of the research on cortical streams focused on the visual domain. However, there is also evidence for the existence of two processing streams in the auditory cortex (Alain et al., 2001; Kaas and Hackett, 1999; Romanski et al., 1999).

1.2. Evidence from the somatosensory domain

Several findings support the hypothesis that streams also characterize cortical somatosensory processing. As in the visual system, multiple full-body somatosensory maps have already been reported in the pioneering studies of Penfield and his colleagues (Penfield and Boldrey, 1937; Penfield and Jasper, 1954; Penfield and Rasmussen, 1950). Later on, studies using electrophysiological recordings in non-human primates and functional neuroimaging in humans extended these results and identified additional somatosensory areas (e.g., Arienzo et al., 2006; Hagen et al., 2002; Ruben et al., 2001; Saadon-Grosman et al., 2020; Sakata et al., 1973; Sereno and Huang, 2006; Young et al., 2004). Moreover, changes in the sizes of receptive fields as well as the level of lateralization in response to somatosensory stimulations have led researchers to posit hierarchical ordering in specific parts of the somatosensory system: rostral to caudal within the post central gyrus (primary somatosensory cortex, S1; (Hyvärinen and Poranen, 1978; Iwamura, 2003, 1998; Iwamura et al., 1993)), S1 to the secondary somatosensory area (S2; (Iwamura, 2003; Mazzola et al., 2005)), S1 to the posterior parietal cortex (Duffy and Burchfiel, 1971; Sakata et al., 1973) and S2 to the posterior insular cortex (Mazzola et al., 2005). In addition, fMRI (Reed et al., 2005; Van Boven et al., 2005) and lesion (Schwoebel and Coslett, 2005) studies reported visual-like anatomical dissociation of somatosensory functions. Integrating a large body of anatomical, as well as behavioral and functional studies, Mishkin proposed serial somatosensory processing from S1 to the insular cortex through S2 as early as 1979 (Mishkin, 1979). Years later, Dijkerman and de Haan further proposed a model for separate cortical somatosensory processing streams, one from S1 to the insular cortex, as suggested by Mishkin, and the other from S1 to posterior parietal cortex (Dijkerman and de Haan, 2007). This latter stream is also supported by differences in onset latencies of cortical areas in response to somatosensory stimulation (Inui et al., 2004; Reed et al., 2009). However, our understanding of the large-scale organization of the somatosensory system has been limited because most of previous studies focused on specific body-parts or on specific cortical areas. In view of the visual streams, we hypothesize the existence of a large scale hierarchical somatosensory organization that is characterized by gradients. To test this hypothesis, we recorded whole brain responses using fMRI to phase-encoded bilateral full-body light touch stimulation. We quantified selectivity, a measure of the specificity of the cortical response to preferred body-parts, and laterality, a measure of the dominance to contralateral response. Incorporating a multi-modal cortical parcellation (Glasser et al., 2016), we defined four gross anatomical regions and computed selectivity and laterality within each region as a function of the distance from the central sulcus (anterior border of the primary somatosensory cortex). We identify somatosensory hierarchical gradients in three anatomically distinct directions: in the parietal lobe, from the central sulcus posteriorly, in the frontal lobe, from the central sulcus anteriorly and in the medial wall, medially to S1 anteriorly and inferiorly.

2. Materials and methods

2.1. Participants

20 participants (age: 27.5 ± 3.33 year-old (mean ± SD), 9 females); all reported no history of neurological, psychiatric, or systemic disorders. All participants provided a written informed consent, and the study was approved by the ethical committee of the Hadassah Medical Center.

2.2. Experimental paradigm

A light-touch somatosensory stimulation was applied to the lips, dorsum part of the hand, forearm, upper arm, shoulder, trunk (lateral part), hip (lateral part), thigh (medial part), knee, shin (medial part), the dorsum part of the foot and the toes (Fig. 1A; (Saadon-Grosman et al., 2015, 2020; Tal et al., 2016)). Stimulation was delivered using a 4-cm-wide paintbrush (with extended handle of 0.65 m plastic stick) by an experimenter, trained to maintain a constant pace and pressure. The stimulation was unilateral and continuous (without lifting the brush from the skin), except for one discontinuity between the lips and the hand. To control the timing of the body-part sequence, the experimenter wore fMRI-compatible headphones, delivering preprogrammed auditory cues (Presentation; Neurobehavioral Systems). Stimulation duration was 15 s and the interval between stimulations was 12 s. Each scanning run included 7 repetitions of stimulation of one body side (right/left), followed by 7 repetitions of stimulation of the other body side (left/right). The order (right/left) was counter-balanced between participants. To control for time-order and directionality effect, BOLD activity of each participant was measured in two scanning runs that differed in the order of body-parts stimulations, from lips-to-toes and from toes-to-lips. Run duration was 423 s (282 time repetitions (TRs)), which included a 28.5 s of measurement before the onset of the first repetition and 4.5 s measurement after the last repetition, in addition to 12 s delay between the stimulation of the two body sides.

2.3. Functional MRI image acquisition procedures and preprocessing

All participants were scanned at the same site using a Siemens Skyra 3T system (32-channel head coil) with the same imaging sequence. Blood oxygen level dependent (BOLD) fMRI was acquired using a whole-brain, gradient-echo (GE) echoplanar (EPI) (repetition time (TR)/time echo (TE) = 1500/27 ms, flip angle = 90, field of view (FOV) = 192 × 192 mm, matrix = 64 × 64 (in-plane resolution 3 × 3 mm^2), 26 axial slices, slice thickness/gap = 4 mm/0.8 mm). In addition, high resolution (1 × 1 × 1 mm) T1-weighted anatomical images were acquired to aid spatial normalization to standard atlas space. The anatomic reference volume was acquired along the same orientation as the functional images (TR/TE = 2300/2.98 ms, matrix = 256 × 256, 160 axial slices, 1-mm slice thickness, inversion time (TI) = 900 ms). Preprocessing was performed using the Brain Voyager QX 20.4.0.3188 software package (Brain Innovation) and NeuroElf (http://neuroelf.net), including head motion correction (trilinear interpolation for detection and sinc for correction), slice scan time correction, and high-pass filtering (cut-off frequency, two cycles per scan). Temporal smoothing (FWHM = 4 s) and spatial smoothing (FWHM = 4 mm) were additionally applied. Functional and anatomical datasets for each participant were co-registered and normalized to standardized MNI (ICBM-152) space. All further analyses were performed using in-house custom Matlab (Mathworks, Inc.) scripts.

2.4. Cortical response maps

Each body side was analyzed separately by splitting voxels' time course (137 TR each: 27 s per repetition, 7 repetitions, 1.5 s per TR: 27*7/1.5 = 126 + 8 TRs prior to beginning of stimulation and 3 TRs after stimulation). Voxels' time course were projected on a cortical surface to create a mesh vertex time course (Trilinear interpolation, data in depth along vertex normal from −1 mm to 3 mm of gray-white matter border; FreeSurfer's, fsaverage template brain; (Desikan et al., 2006)). To identify the cortical distribution of the somatosensory system we used a cross correlation analysis (Saadon-Grosman et al., 2020, 2015). A boxcar function (3 s) was convolved with a two-gamma hemodynamic response function (HRF), to derive a predictor for the analysis. This predictor and the time course of each vertex were cross-correlated to measure responses to different parts of the stimulation cycle (body-parts). The first

TR in the stimulation block was excluded to avoid time-order and directionality effects. The predictor was cross correlated across all TRs in the block, except for the last one, to allow averaging of the two opposite stimulation directions ("start lips" and "start toes"). Stimulation duration of each cycle consisted of 10 TRs, thus, cross correlation analysis produced 8 correlation values for each vertex, indicating correlation to different parts of the stimulation cycle.

Each TR can be assigned to a specific body part by its stimulation time. However, this is not used in this study except as a control in Fig. 6 (dark gray). Group maps were computed with two level statistics random effect: to combine the correlation distributions of start lips and start toes directions, we flipped the order of the correlation values of the start toes paradigm and then averaged over the two directions. The 8 resulting correlation coefficients (corresponding to 8 cross correlation lag values for each vertex of each participant) were transformed to t values with: $t = r \cdot \sqrt{\frac{n-2}{1-r^2}}$ where n is the sample size (number of measurements-TR, 137). We then applied a vertex wise one tailed t-test ($H_0: \mu = 0$, $H_1: \mu > 0$) on the t-values from all participants for each lag separately. The resultant p values were corrected for spatial multiple comparisons with the Benjamini-Hochberg false discover rate (FDR; (Benjamini and Hochberg, 1995)). The final group map (Fig. 1B) was comprised from t-values corresponding to the lowest p value in each vertex (out of 8) masked with significance threshold of α=0.05 Bonferroni-corrected for 16 comparisons (cross correlation with 8 lags in two stimulation directions).

2.5. Selectivity

To quantify the selectivity of the response of each vertex to a TR (corresponding to a body part), we computed the width of the vertex's tuning-curve. At first, each vertex's time course was normalized (z-score) to compute an event related averaged response (ERA) across all stimulation cycles. ERA is computed by averaging responses across time windows (18 TRs each, compose of 10 TRs of stimulus block and 8 TRs of baseline rest) across 7 repetitions. Since stimulation was applied continuously over the whole body, the ERA depicts the response tuning curve (degree of selectivity to a specific body-part). To measure the width of each vertex's tuning curve we fitted a Gaussian curve and extracted the distribution's standard deviation using the fitted Gaussian coefficients (Fig. 2A). The fitted curve is given by Eq. (1) where the x denotes TRs of the ERA response, σ standard deviation and μ is the mean.

$$f(x) \propto e^{-\frac{1}{2}\left(\frac{x-\mu}{\sigma}\right)^2} \tag{1}$$

Selectivity s, was defined as $s = 1/\sigma$. It should be noted that because our focus is a comparison of selectivity between regions, and the absolute value of selectivity is immaterial, we did not commit to a specific HRF and did not take into account the shape of the function, this is unlike (Dumoulin and Wandell, 2008; Harvey et al., 2013; Puckett et al., 2020; Schellekens et al., 2018).

Only those vertices that proved significant in the random effect response group map, corrected for multiple spatial comparisons (FDR), were considered (Fig. 1B). For those vertices, group selectivity was computed by averaging selectivity (s) across all participants and across two stimulus directions (lips-to-toes and from toes-to-lips) that (1) exhibited significant response in that vertex, determined by maximal correlation of prediction (t-test, $\alpha = 0.01$, Bonferroni corrected for multiple correlations; 8 lag values, $p < 0.0013$, a procedure that removed 26% of the vertices x participants x stimulus directions) and (2) their ERA was well-fitted by a Gaussian (R^2=residual sum of squares/total sum of squares; $R^2 > 0.6$, a procedure that removed 24% of the remaining vertices x participants x stimulus directions). Qualitatively similar results were obtained for $R^2 > 0.28$, a procedure that removed only 10% of the remaining vertices x participants x stimulus directions. These criteria were chosen to avoid noise contamination

2.6. Laterality

Laterality was defined as the preference of a given vertex to stimulation of the contra- or ipsi-lateral body-side. It is denoted by the normalized difference between the maximal responses (maximal cross correlation with predictor) to stimulation of the contra- and ipsi-lateral body sides (Eq. (2)).

$$l = \frac{C_{contra} - C_{ipsi}}{C_{contra} + C_{ipsi}} \tag{2}$$

Positive values indicate a contralateral preference and negative values indicate an ipsilateral preference. Only those vertices that proved significant in the random effect response group map, corrected for multiple spatial comparisons (FDR), were considered (Fig. 1B). For those vertices, group laterality was computed by averaging laterality (l) across all participants and across two stimulus directions that exhibited significant response in that vertex (to avoid noise contamination), determined by maximal correlation of prediction to stimulation in either the contra or ipsilateral sizes (t-test, $\alpha = 0.01$, Bonferroni corrected for multiple correlations; 8 lag values × 2 sides, $p < 0.0006$, a procedure that removed 16% of the vertices x participants x stimulus directions).

2.7. Cortical parcellation and identification of somatosensory responsive areas

In this study we applied a multi-modal data-driven parcellation (Glasser et al., 2016). This parcellation delineates 180 areas per hemisphere, bounded by sharp changes in cortical architecture, function, connectivity, and/or topography (Glasser et al., 2016). Parcellation areas containing more than 50% of vertices responding to body stimulation (group mask) were defined as somatosensory responsive areas (Table S1). This threshold was used to eliminate areas which did not pass majority rule (i.e. areas with less than 50% significant vertices). In those parcellation areas, only those responding vertices were included in the analysis.

To calculate selectivity and laterality of a given parcellation area, we averaged the computed values for all vertices of all participants that passed the exclusion criteria (as a result, the contribution of different participants to selectivity and laterality of a parcellation area was not equal).

2.8. Selectivity and laterality as a function of distance from the central sulcus

We quantified selectivity and laterality with respect to the distance from the central sulcus, the anterior border of the primary somatosensory cortex. To determine a distance along the cortical surface, we calculated the minimum geodesic distance by using an algorithm that approximates the exact distance along the shortest path between two vertices on a triangular surface mesh (Mitchell et al., 1987) (Geodesic computation package by Danil Kirsanov (https://code.google.com/archive/p/geodesic/), a set of MATLAB functions by Yanir Kleiman and Maks Ovsjanikov, CGF 2018). The surface used was the "midthickness" surface, an average between the pial and white matter surfaces. We looked for the shortest path from each vertex to area 3a, which is bounded anteriorly by the central sulcus. For vertices within area 3a, the distance is, by definition, zero. For clear visualization we averaged selectivity and laterality within 10 quantiles of the geodesic distance within each region of interest. For group analysis we used the above described selectivity and laterality group maps (2.5,2.6). Error bars were computed by bootstrapping over participants (1000 iterations; standard deviation).

2.9. Gross-anatomy classification

The somatosensory system as found here lies over four gross anatomical regions, including the anterior part of the parietal lobe (from Brod-

mann area (BA) 3a to the ventral and medial intraparietal areas (BA 7)), the posterior part of the frontal lobe (from BA 4 to the anterior end of BA 6), the superior part of the medial wall (from the medial end of the pre and post central gyri to the middle cingulate gyrus) and the operculum-insular cortex (from parietal and frontal operculum to temporal operculum through the posterior insula). In order to define these regions precisely we utilized the above mentioned parcellation. We classified each of the somatosensory parcellation areas according to the following criteria: the parietal region includes all areas on the lateral surface posterior to the central sulcus, the frontal region includes all areas on the lateral surface anterior to the central sulcus, the medial region includes all areas on the medial wall, and the operculum-insula region includes areas inferior to the parietal and frontal lobes of the operculum and insular cortex (Table S1, (Glasser et al., 2016)). Note that areas 4, 6mp, 5 L and 7Am (Glasser et al., 2016) on the lateral surface extend into the medial wall. Additional parcellation areas that were not included in these anatomical regions as part of the spatial continuous representation were not considered in the analysis (13 in the right hemisphere and 8 in the left hemisphere, see Table S1). Specifically, the distance-dependence selectivity and laterality depicted in Fig. 5 incorporated the above four regions.

2.10. Specific controls

To exclude the possibility that changes in selectivity and laterality reflect heterogeneities in the signal to noise ratio (SNR) or differences in body parts spatial distributions we spatially permuted selectivity and laterality of the contralateral response across the entire contralateral somatosensory responsive cortex in two ways: (1) functional SNR was computed by vertex-wise averaging of all correlation pairs of the BOLD responses across the seven stimulus repetitions in each participant and each stimulus direction (as a measure of variability in response). Then, we permuted all vertices sharing the same functional SNR (using 20 bins) and re-computed selectivity and laterality with distance from the central sulcus (light gray in Fig. 6). (2) Same as in (1) for all vertices sharing the same preferred body part (8), defined by the maximum of the cross-correlation analysis (dark gray in Fig. 6).

2.11. Data and code availability statement

All data is publicly available at: https://openneuro.org/datasets/ds003089/versions/1.0.1. Code related to analyses in this study is available on GitHub (https://github.com/CompuNeuroPsychiatryLabEinKerem/publications_data/tree/master/Somatosensory_hierarchical_gradients).

3. Results

We applied whole-body continuous tactile stimulation to 20 participants while measuring BOLD responses using fMRI (Fig. 1A). We identified vertices in which the response to contralateral body side stimulation was significant (random effect, $\alpha = 0.05$, FDR corrected, see Methods 2.4). This defined a somatosensory response map that includes S1, S2, M1, SMA, premotor cortex, anterior part of the superior and inferior parietal lobules, posterior insular and mid cingulate cortex (Fig. 1B).

3.1. Selectivity

Interested in hierarchical somatosensory processing, we quantified vertices' selectivity. To that end, we considered, for each participant and for each stimulation direction, the contralateral event-related average response (ERA) of each vertex (see Methods 2.5 and Fig. 2A). Because body-parts' stimulation is continuous and its order is fixed, this ERA is analogous to a tuning curve. Thus, the reciprocal of the width of the ERA (denoted by s) is a measure of selectivity (see Methods 2.5 and Fig. 2B). Fig. 2C depicts the group-averaged selectivity across the contralateral

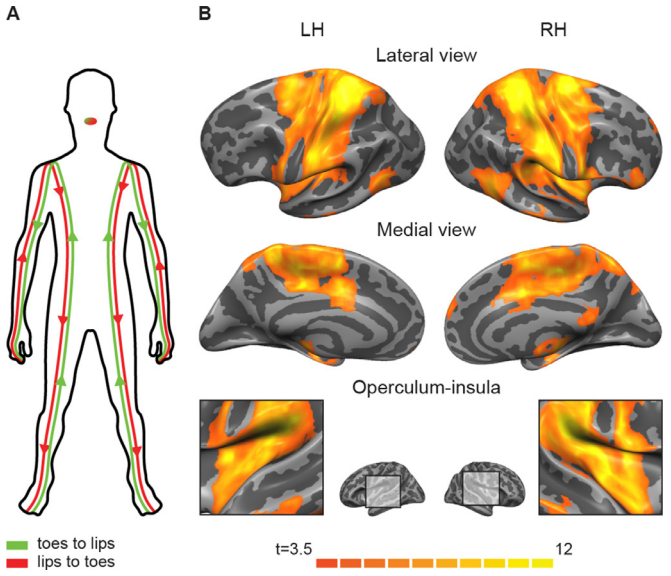

Fig. 1. Experimental paradigm and somatosensory response map. **A.** Experimental paradigm: Scheme of bilateral whole-body continuous brush movement from lips-to-toes (red) and from toes-to-lips (green). **B.** somatosensory response maps: random effect group maps ($N = 20$; see Methods 2.4) of contralateral body side stimulation. Top, Lateral view, Middle, Medial view; Bottom, operculum and insula cortices (LH: left hemisphere; RH: right hemisphere; $\alpha = 0.05$, corrected for spatial multiple comparisons (FDR) and multiple correlations (Bonferroni), see Methods 2.4).

somatosensory-responsive cortex (for ipsilateral selectivity maps see Fig. S1, see also Fig. S2). Selectivity is highest in the rostral part of S1 and M1 and lower selectivity is observed in association cortices.

3.2. Laterality

Laterality is another measure of processing hierarchy. To quantify it, we used, for each participant and for each stimulation direction, the correlation coefficients between the BOLD responses in each vertex and its predictors based on stimulation of the two body sides (Fig. 3A, see methods 2.6). We defined laterality index l as the difference between the contralateral and ipsilateral maximal correlation coefficients, divided by their sum (see Methods 2.6, Fig. 3B). As with selectivity, the most contralateral response was found in the primary cortices S1 (rostral part) and M1 while robust bilateral responses were found in the posterior part of the parietal, anterior part of the frontal and anterior insular somatosensory cortex (Fig. 3C, see also Fig. S2).

3.3. Selectivity and laterality are correlated

Considering both selectivity and laterality as measures of hierarchy, these measurements should be correlated. This hypothesis is tested in Fig. 4, which depicts the laterality as a function of the selectivity at the level of the single vertex in the entire somatosensory responsive cortex. The two measures were found to be highly correlated (correlation coefficients $r = 0.76,\ N = 47,863,\ p = 0$ and $r = 0.56,\ N = 61,128,\ p = 0$ for the left and right hemispheres, respectively).

3.4. Hierarchical gradients

If the somatosensory cortical system is hierarchically organized, then we expect both selectivity and laterality to decrease as we move away from the primary somatosensory cortex. Therefore, we measured how average selectivity and laterality change as we move away from the central sulcus (the anterior border of S1). We found that indeed, both selectivity and laterality significantly decrease with the geodesic distance from the central sulcus ($p < 0.001$, Fig. 5, see also Methods).

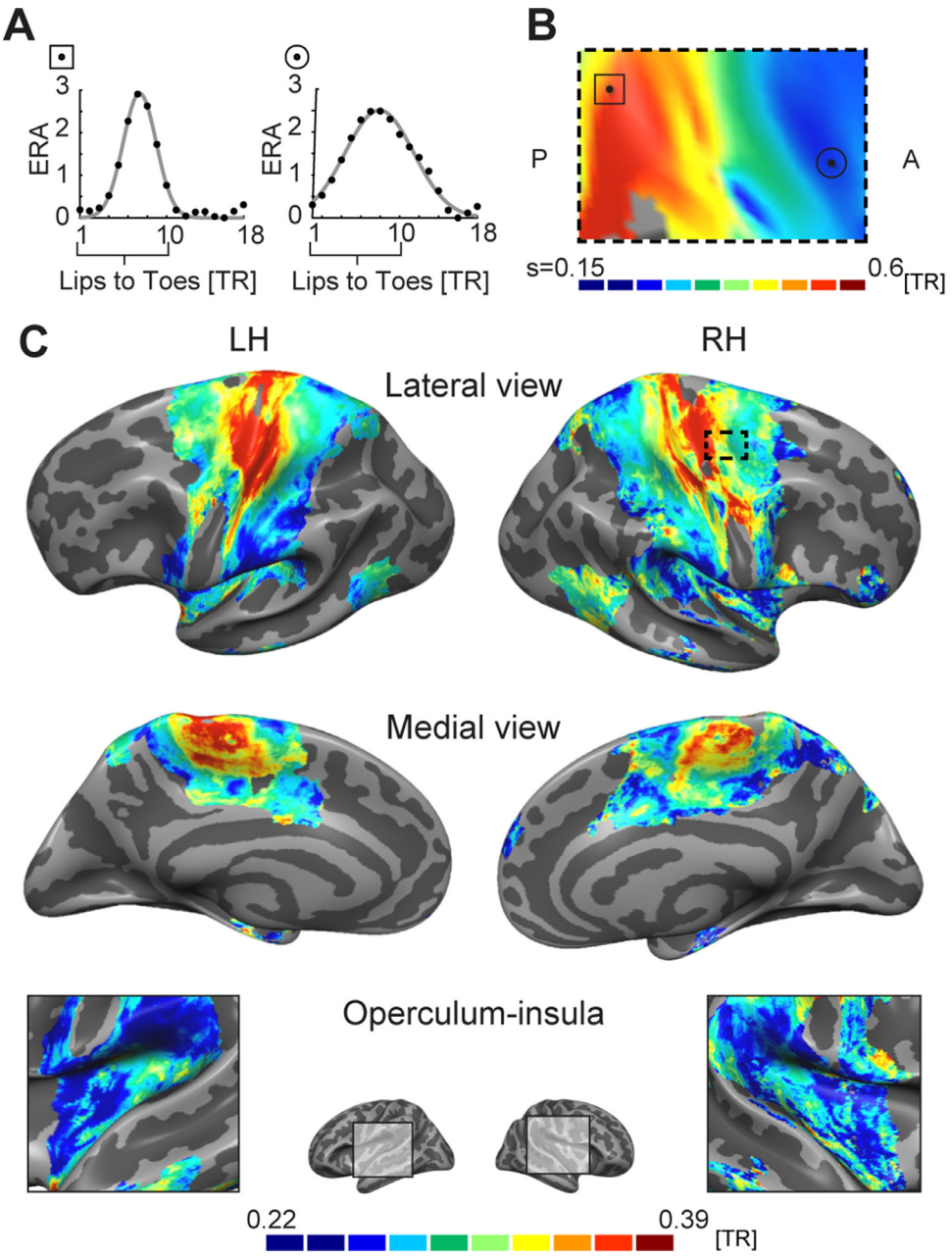

Fig. 2. Selectivity across the somatosensory responsive cortex. **A.** Selectivity of two representative vertices. Dots, the contralateral ERA, averaged response over seven repetitions of lips-to-toes stimulation (TRs 1–10) of a single participant. Line, best-fit Gaussian. **B.** Selectivity of part of the posterior-frontal cortex of the right hemisphere of the participant in A. For each vertex, a selectivity measure, the reciprocal of the standard deviation of the best-fit Gaussian was computed and is presented in color code (A- anterior; P-posterior). The vertex examples in A are denoted by square (left, PA 4, high selectivity) and a circle (right, PA 6a, low selectivity). **C.** Group selectivity maps. (LH: left hemisphere; RH: right hemisphere; see also Fig. S3). Vertex-selectivity was computed by averaging the selectivity across all participants and two stimuli directions that exhibited significant response ($\alpha = 0.01$, Bonferroni corrected for multiple correlations) and that their ERA was well-fitted by a Gaussian ($R^2 > 0.6$, see Methods). The location of the patch in B is marked by a dashed rectangle.

3.5. Processing directions

The somatosensory system as found here lies over four anatomically distinct regions: (1) parietal lobe, (2) frontal lobe, (3) operculum and insular cortex and (4) the medial wall, where the primary somatosensory cortex resides at their intersection. This motivated us to ask whether these different cortical regions correspond to different somatosensory processing directions. We used a cortical parcellation (Glasser et al., 2016) to draw the borders between the four regions (Fig. 6, top; Methods 2.9, see also Table S1). Within each region, we measured how average selectivity and laterality change as we move away from the central sulcus (for single participants see Fig. S4).

3.5.1. Parietal

Moving posteriorly in the parietal direction, from the central sulcus through S1 to the posterior parietal cortex, we found a significant decrease in both selectivity and laterality (Fig. 6A bottom; LH: $p < 0.001$, RH: $p = 0.001$, bootstrapping over participants). We suggest that the previously-reported rostral to caudal hierarchy within S1 (Iwamura et al., 1993) and the hierarchy between S1 and posterior parietal cortex (Sakata et al., 1973) are both part of a continuous processing direction.

3.5.2. Frontal

The frontal direction, anteriorly from the central sulcus, starts in the primary motor cortex and ends in premotor areas (Fig. 6B, top). As in the parietal direction, selectivity and laterality decrease significantly and monotonically along the frontal direction (Fig. 6B bottom; $p < 0.001$, bootstrapping over participants).

3.5.3. Medial

The medial region spreads from right medially to S1 (posteriorly to the medial end of M1) and reaches the mid cingulate cortex through the paracentral lobule (Fig. 6C, top). Both selectivity and laterality significantly decrease in the medial direction (Fig. 6C bottom; Selectivity- RH: $p = 0.005$, LH: $p < 0.001$; Laterality- RH: $p = 0.003$, LH: $p < 0.001$,

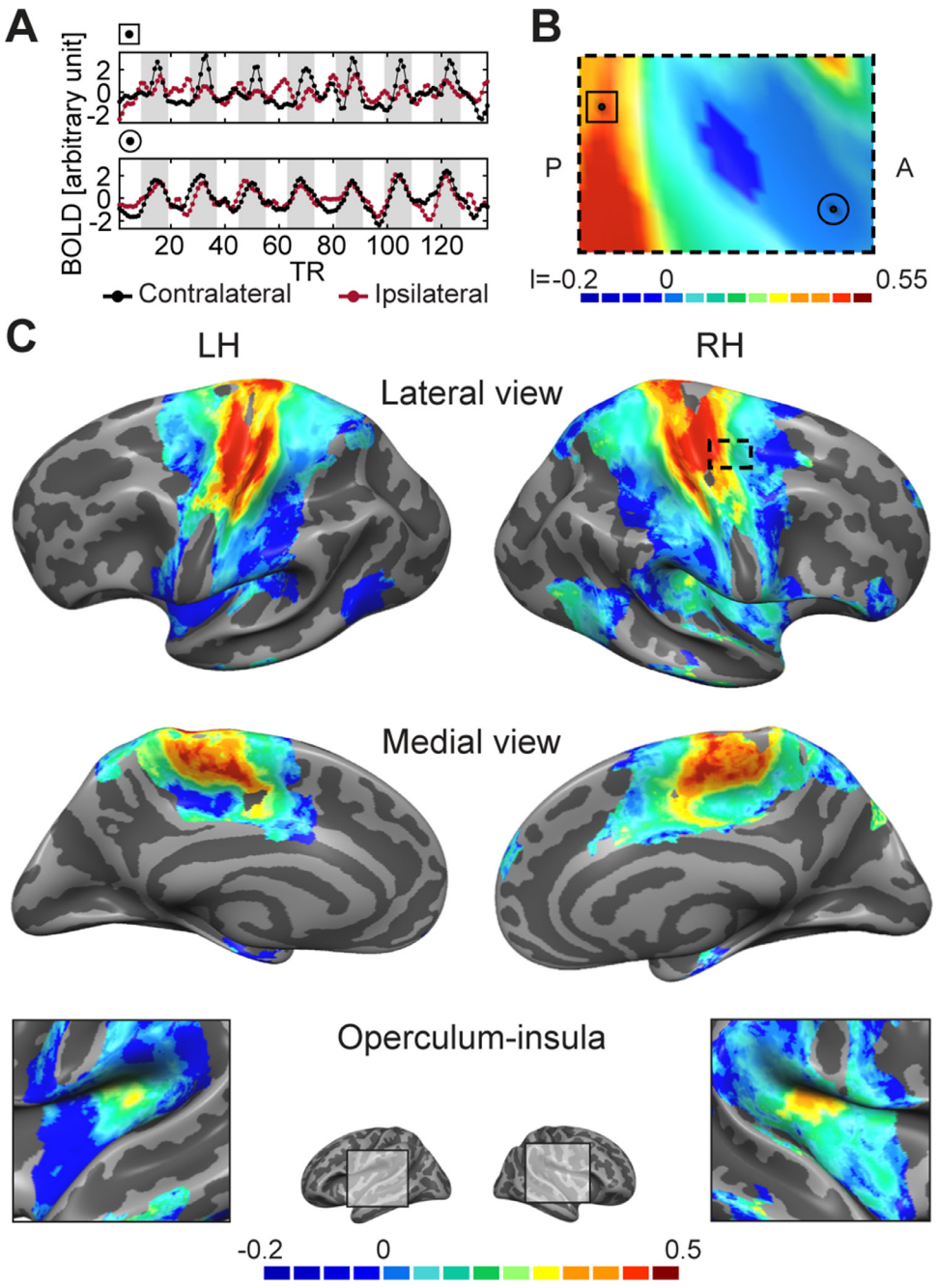

Fig. 3. Laterality across the somatosensory responsive cortex. **A.** Examples of normalized BOLD responses of a single participant in two representative vertices (top and bottom) in response to seven repetitions of contralateral (black) and ipsilateral (red) Lips-to-Toes stimulation. Gray and white strips denote stimulation and rest periods, respectively. Laterality in the upper plot is high: the BOLD response closely follows the contralateral, but not the ipsilateral stimulation. By contrast, laterality in the bottom plot is low: the response to both contralateral and ipsilateral stimulations is similar. **B.** Laterality, defined as the difference between the contralateral and ipsilateral maximal correlation coefficients (between the BOLD response in each vertex and its stimulus-based predictors), divided by their sum, of the participant in A is presented in color code (A-anterior; P-posterior). The vertex examples in A are denoted by square (top, PA 4, high laterality) and a circle (bottom, PA 6a, low laterality). The parameter l can range between −1 and 1. While $l = 1$ denotes a pure contralateral preference and $l = 0$ corresponds to a bilateral response. **C.** Group laterality maps. (LH: left hemisphere; RH: right hemisphere; see also Fig. S3). Vertex-laterality was computed by averaging the laterality across all participants and two stimuli directions that exhibited significant response ($\alpha = 0.01$, Bonferroni corrected for multiple correlations). Note that the location of the map patch in B is marked with a dashed rectangle.

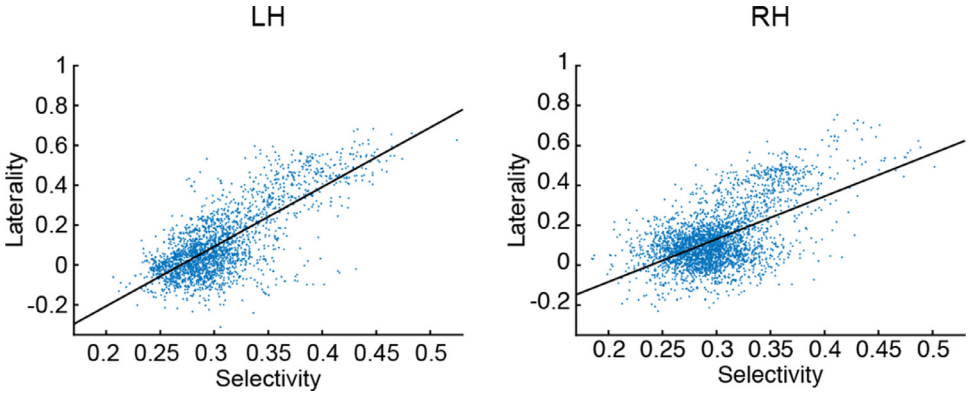

Fig. 4. Selectivity and laterality are correlated. The laterality of the vertices depicted as a function of their selectivity. Each dot corresponds to a single vertex that met the significance criterion (as in Figs. 2C and 3C) and for reasons of visual clarity, only 5% of the vertices, randomly selected, are depicted. Black lines are linear fits ($r = 0.76$ and $r = 0.56$ for the left (LH) and right (RH) hemispheres, respectively).

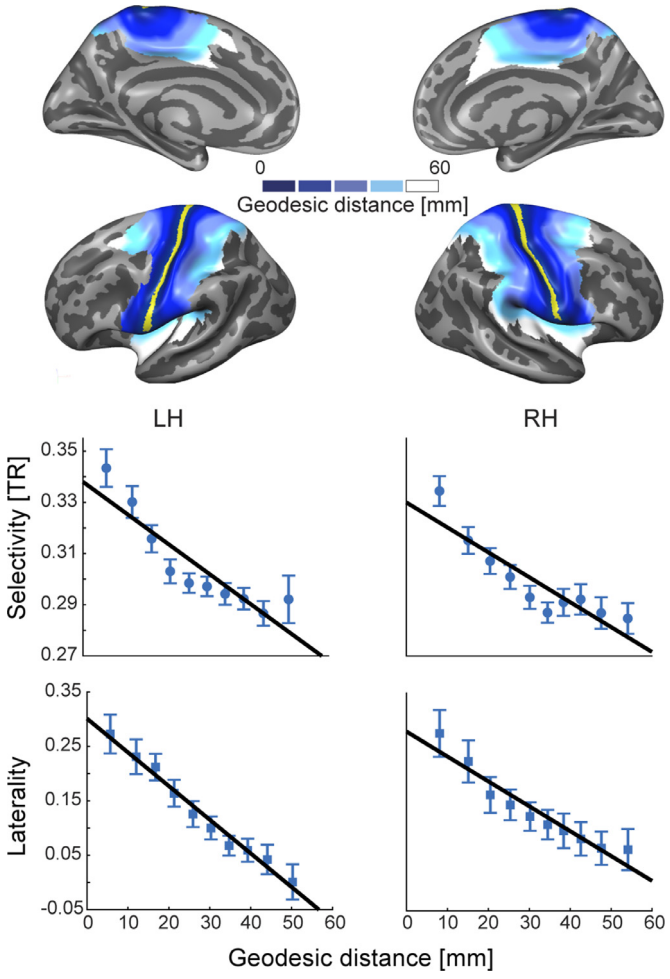

Fig. 5. Selectivity and laterality decrease with the distance from the central sulcus. Lateral and medial views of the left and right hemispheres (LH, RH; top). Color code represents the geodesic distance in millimeters of each vertex from area 3a (posterior to the central sulcus, marked in yellow). Middle, average selectivity; Bottom, average laterality within 10 distance quantiles. Black lines denote linear regression. The negative slope in all of them is significantly different from zero ($p < 0.001$). Error bars are standard deviation, computed by bootstrapping over participants.

bootstrapping over participants). However, the magnitude of the change (slope) is smaller than that in the parietal and frontal directions (Table S2). Note that the selectivity and laterality at the starting point of this direction are both small relative to the starting points of the parietal and frontal directions.

3.5.4. Operculum-insula

The Operculum region covers parts of the frontoparietal opercula (inferiorly to M1, S1 and the inferior parietal lobule, including S2), posterior insula and the temporal opercula (Fig. 6D, top). In contrast to the three other directions, we observe significant increase of selectivity (Fig. 6D bottom; RH: $p = 0.024$, LH: $p = 0.002$, bootstrapping over participants) and decrease of laterality (RH: $p = 0.003$, LH: $p = 0.001$, bootstrapping over participants) with distance from the central sulcus.

3.6. Controls

We argue that the descending gradients in selectivity and laterality as we move away from the central sulcus are indicative of a processing direction. However, before accepting this interpretation, we should consider alternative explanations. One possibility worthwhile considering is that the change in selectivity and laterality reflect differences in signal-to-noise ratio (SNR) across different cortical areas. The reason is that the selectivity and the laterality of a response that is dominated by noise is expected to be low. Thus, a decrease in the selectivity and laterality as we move away from primary regions could, in principle, reflect a reduction in the SNR. To control for this possibility, we used the correlation across stimulus repetitions as a measure of the functional SNR (see Methods 2.10). For each participant and each direction, we permuted all vertices, while maintaining the spatial distribution of the functional SNRs. We used this surrogate data to recompute the change in the selectivity and laterality along the four directions. As shown in Fig. 6 (light gray), a change in the functional SNR cannot account for the change in selectivity and laterality.

Another alternative explanation could have been that the gradients reflect changes in the representations of different body parts along the different directions (Saadon-Grosman et al., 2020). For example, it is known that the face and the trunk are more bilaterally represented than the limbs (Eickhoff et al., 2008; Killackey et al., 1983). Thus, a decrease in the representation of the limbs along a direction is expected to result in a decrease in laterality. To control for this, we associated each vertex of each participant and each stimulus direction with its preferred body part (see Methods 2.10). For each participant and for each direction, we permuted all vertices, while maintaining the spatial distribution of the body-parts representation. We used this surrogate data to recompute the change in the selectivity and laterality along the four directions. As shown in Fig. 6 (dark gray), a change in the distribution of body-parts representation cannot account for the change in selectivity and laterality.

4. Discussion

4.1. Summary

In this study we measured BOLD signals in response to whole body light touch stimulation. We defined two measures of cortical response, selectivity and laterality. Both were found higher in primary somatosensory and motor cortices while lower in association cortices. This result, is reminiscent of the electrophysiological findings that the receptive fields are more lateralized and sharply-tuned (selective) in primary regions than in higher processing regions (Hubel and Wiesel, 1962; Iwamura, 2003; Kaas et al., 1979). We used selectivity and laterality to characterize processing hierarchy in the somatosensory-responsive cortex. This analysis enabled us to identify three anatomically distinct somatosensory hierarchical gradients. In the parietal lobe, from the central sulcus posteriorly, in the frontal lobe, from the central sulcus anteriorly and in the medial wall, medially to S1 anteriorly and inferiorly. In view of the anatomical segregation of these three directions, the multiplicity of body representations in each region (Huang and Sereno, 2018; Saadon-Grosman et al., 2020) and the hierarchy in our findings, we propose that as in the visual domain, these directions are, in fact, *streams* of somatosensory information processing.

4.2. From selectivity and laterality through hierarchical gradient(s) to processing streams

The experimental results are consistent with the general increase in hierarchy as we move away from central sulcus (Fig. 5). We would like to propose a possible interpretation of this data based on multiple processing streams (Fig. 6). As described in the Introduction, three lines of evidence support the cortical streams hypothesis in the visual domain: (1) functional dissociation, (2) multiple maps and (3) hierarchy. Regarding hierarchy, we used the fMRI analog of a receptive field. We followed the path of electrophysiologists, which measured the selectivity and laterality of single neurons as proxies for the hierarchical processing level (e.g., Hubel and Wiesel, 1962; Iwamura et al., 1993; Sakata et al.,

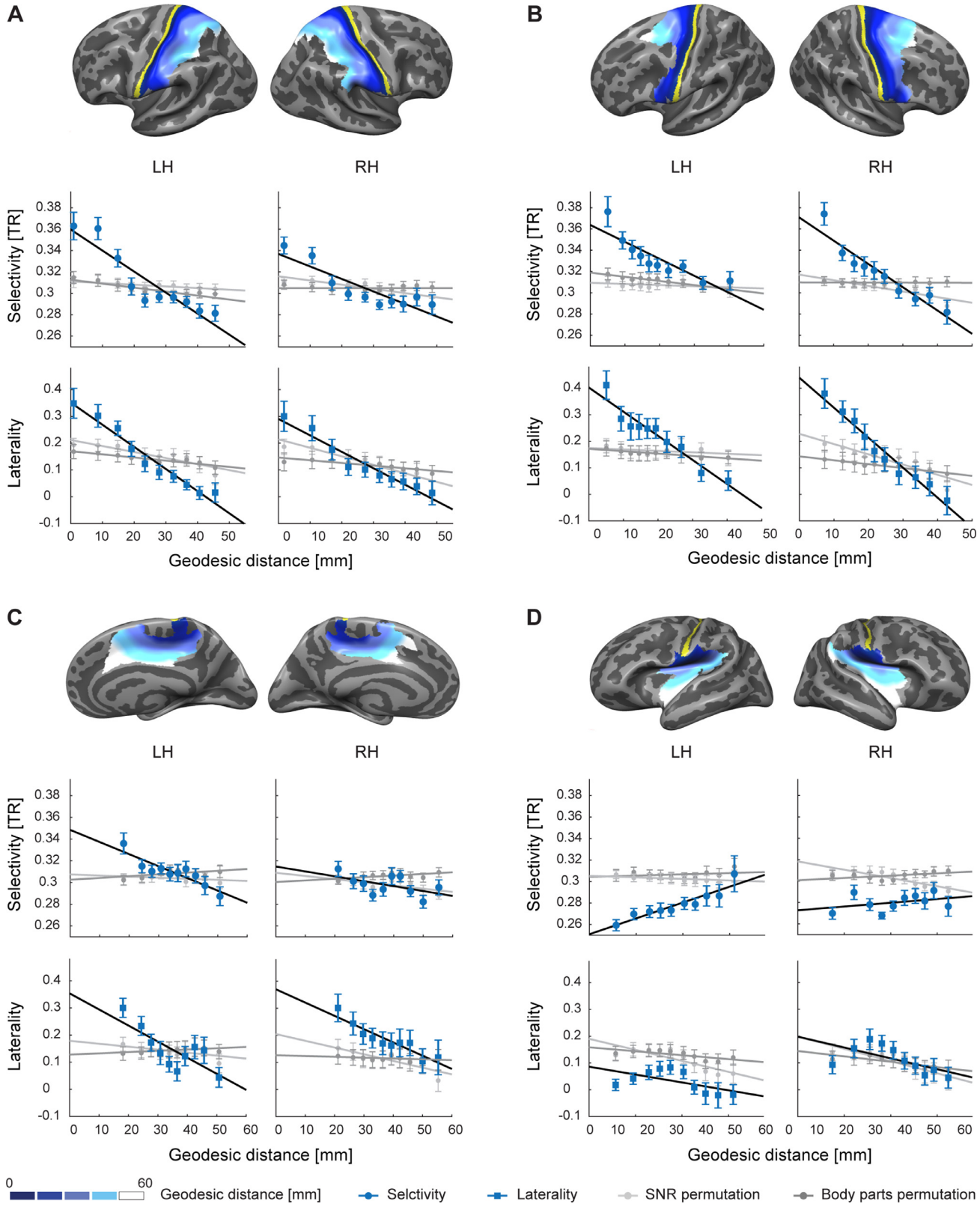

Fig. 6. Somatosensory hierarchical gradients. Four gross anatomical regions, **A.** parietal, **B.** frontal, **C.** medial and **D.** operculum-insula are denoted on the right and left hemispheres (RH, LH; top). Color code represents the geodesic distance in millimeters of each vertex from area 3a (posterior to the central sulcus, yellow). Middle, average selectivity; Bottom, average laterality within 10 distance quantiles. Black lines denote linear regression. In gray, controls for functional SNR (light gray) and body-parts' distribution (dark gray). Error bars are standard deviation, computed by bootstrapping over participants.

1973), and measured changes in selectivity and laterality at the population level. We found that in the parietal and frontal directions, and to lesser degree in the medial direction, but not in the operculum-insula, selectivity and laterality decrease as we move away from the central sulcus. With respect to multiple maps, previous studies have demonstrated the existence of multiple body maps in each of the processing directions (Arienzo et al., 2006; Hagen et al., 2002; Huang and Sereno, 2018; Kaas, 2004; Penfield and Jasper, 1954; Saadon-Grosman et al., 2020). With respect to functionality, the extent to which somatosensory information is functionally dissociated is still unclear and a proof of a functional dissociation between the three directions awaits future experiments.

4.3. Processing directions

4.3.1. The parietal direction

Previous studies have provided evidence of somatosensory hierarchies in parts of the parietal cortex. Within S1 (Brodmann areas 3a,3b,1 and 2), single-unit recordings in non-human primates demonstrated an increase in the complexity of receptive field properties and integration of bilateral sides of the body along the rostral-caudal (anterior to posterior) axis (Hyvärinen and Poranen, 1978; Iwamura, 2003; Iwamura et al., 1993). In agreement with these results, BOLD responses in area 3b were found to be more selective than those in area 1 (Ann Stringer et al., 2014). Moreover, response latencies to somatosensory stimuli were longer in area 1 than in areas 3 (Inui et al., 2004). Finally, the existence of this processing direction within S1 is also supported by anatomical evidence of serial corticocortical connections (Felleman and Van Essen, 1991).

Posterior to S1, there is substantial evidence that both Brodmann areas 5 and 7 are higher in the processing hierarchy than S1. First, electrophysiological recordings reveal that neurons in area 5 respond to multiple body parts. Moreover, neurons with ipsilateral and bilateral receptive fields were found in these areas (Sakata et al., 1973; Taoka et al., 1998). Also, the receptive fields of neurons in Brodmann area 7 are larger than those in S1 (Leinonen et al., 1979; Robinson and Burton, 1980). Second, response latencies in area 5 are longer than in S1 (Hayashi et al., 1995; Inui et al., 2004). Together, these results indicate that areas 5 and 7 are higher in the processing hierarchy than S1. Our findings generalize these results, demonstrating that the hierarchies within S1 and between S1 and areas 5 and 7 reflect a single organization principle – a processing direction that originates in the anterior part of S1 and extends in the parietal direction.

4.3.2. The frontal direction

In comparison with the parietal direction, the evidence in the literature supporting a somatosensory frontal processing direction is limited. There is anatomical evidence of projections from M1 to the premotor cortex (Felleman and Van Essen, 1991). Evidence for processing hierarchy in the frontal direction comes from the finding that sensory processing in premotor areas (but not in M1) is multimodal (Graziano et al., 1994; Murata and Ishida, 2007; Rizzolatti et al., 2002).

Most studies on the posterior-frontal lobe focused on its role in motor control (Graziano, 2006). The motor processing direction in this area is primarily processed from premotor areas to the primary motor cortex (M1; (Fuster, 1993; Kandel et al., 2000)), opposite to our finding of a somatosensory hierarchy from M1 to premotor areas. Together, these results indicate that sensory and motor information are processed in opposite directions. The existence of two processing streams in opposite directions may seem counterintuitive. However, we argue that sensory and motor streams are expected to be opposite. The gross planning of a motor sequence (likely to occur in premotor areas) requires large-scale somatosensory information whereas the actual execution of the motions requires more detailed information about specific body parts.

4.3.3. The medial direction

Most parts of the medial region are considered as higher-level motor areas (Deiber et al., 1996; Lee et al., 1999; Rolanc and Zilles, 1996). Nevertheless, somatosensory responses were recorded in the paracentral lobule and in the middle cingulate gyrus (Arienzo et al., 2006; Kaas, 2004; Penfield and Jasper, 1954). Moreover, somatosensory responsive neurons with large receptive fields were found in the medial wall (Kaas, 2004). We observe substantial somatosensory responses in the medial region, with selectivity and laterality decreasing as we move away from the medial end of S1 to the cingulate cortex. Compared with the parietal and frontal directions, the modulation of these measures is relatively small (Table S2). A possible interpretation is that while both the parietal and frontal regions includes primary cortices whose selectivity and laterality is highest, the medial direction starts in association cortex. When considering Figs. 2C and 3C, selectivity and laterality are maximal in the medial part of the primary motor area (M1, area 4) and decrease as we move away from M1. An alternative definition of the medial region that includes M1 or part of it would result in a larger modulation of selectivity and laterality.

4.3.4. The operculum-insula

We did not identify a somatosensory hierarchical gradient in the operculum-insula that originates in the central sulcus. This, however, does not imply that selectivity and laterality are homogeneous in this region. Rather, we observe in Figs. 2C and 3C that peak laterality and to a lesser extent that selectivity is higher within S2 and are lower around it. This could indicate a processing stream that originates in S2. Indeed, hierarchy between S2 and the insula has been previously suggested (Friedman et al., 1986; Mazzola et al., 2005). Another interpretation could be that the hierarchical structure in this region is different, perhaps more complex. In this work, based on previous studies, hierarchy was demonstrated with a decrease in both selectivity and laterality. We showed that these two measurements are correlated in the somatosensory responsive cortex. Examination of the relationship between selectivity and laterality in each one of the four gross anatomical regions separately (Fig. S5) points on an interesting finding. While in the Parietal, Frontal and Medial regions the correlation is extremely high (Parietal- $r_{LH} = 0.87$, $r_{RH} = 0.73$; Frontal- $r_{LH} = 0.8$, $r_{RH} = 0.75$; Medial- $r_{LH} = 0.69$, $r_{RH} = 0.6$; all p's=0) in the Operculum-insula region it is rather small ($r_{LH} = 0.29$, $r_{RH} = 0.1$; p's=0). This might suggest that a different processing principle governs the operculum-insula region.

4.4. Macroscale gradients and somatosensory processing directions

The focus of this work was the changes in the responses to somatosensory stimulations as we move away from the central sulcus along the cortical surface. Previous studies, however, have demonstrated that responses also become less selective to the somatosensory modality, changing from unimodal selectivity to multimodal selectivity (Mesulam, 1998). For example, the visual dorsal stream terminates in the posterior partial cortex, and regions there are selective to both visual and somatosensory stimuli (Sereno and Huang, 2014). These observations raise the question of how the somatosensory responsive cortex is integrated within the larger scale organization of the cortex. Resting state fMRI analysis revealed that the macroscale cortical structure is characterized by conserved spatial order of functional networks (Power et al., 2011) that is repeated along the cortical surface, from perception and action to more abstract cognitive functions (Margulies et al., 2016).

Interestingly, the three processing directions identified in this study are spatially aligned along three of the gradients identified in that study. We thus hypothesize that the somatosensory processing directions identified here are part of the larger scale functional organization of the cortex.

4.5. Limitations

Our analysis was based on a particular segmentation of the parcellation areas to the four gross anatomical regions (Glasser et al., 2016). While the segmentation of most parcellations areas is indisputable, four parcellation areas constitute of both medial and lateral parts: area 5L, 7Am, 6mp and area 4. Most of area 4 (M1) and most of area 6mp reside in the lateral part and therefore they were taken as part of the frontal region. With respect to areas 5L and 7Am, both are almost equally divided between the medial and lateral regions. The medial region originates in the medial end of S1 and stretches anteriorly and inferiorly towards the cingulate gyrus. Both areas 5L and 7Am are located posteriorly to the medial end of S1, rather than anteriorly and inferiorly. Therefore, we associated both to the lateral parietal region, and not to the medial region. It should be noted, however, that including them in the medial region does not have a qualitative effect on our results. A second limitation of our study is that it is difficult with current data to reliably identify the borders between the multiple dissociated body maps and thus to arrange them based on their average selectivity and laterality. Finally, there could potentially be alternative accounts explaining the reported somatosensory hierarchical gradients. For example, spatial variability introduced by co-registration of multiple individuals could explain the decrease in selectivity and laterality moving away from the central sulcus. To address this and other alternative explanations, we repeated the analysis for each participant and each stimulus direction separately. The decrease in selectivity and laterality along the three directions is evident also at the single participant level (Fig. S4).

4.6. Conclusion

Three hierarchical gradients in cortical somatosensory processing were introduced by the quantification of selectivity and laterality of response to whole body light touch stimulation. We suggest that similar to the well-known visual domain, these gradients represent somatosensory streams. Furthermore, we speculate that the somatosensory streams are part of the larger scale functional gradient organization of the cortex.

Funding

This work was supported by The Israel Science Foundation (Grants No. 757/16, 1306/18) and the Gatsby Charitable Foundation.

Declaration of competing interest

None.

CRediT authorship contribution statement

Noam Saadon-Grosman: Conceptualization, Data curation, Formal analysis, Investigation, Methodology, Project administration, Resources, Software, Validation, Visualization, Writing - original draft, Writing - review & editing. **Shahar Arzy:** Conceptualization, Data curation, Formal analysis, Funding acquisition, Methodology, Project administration, Resources, Software, Supervision, Validation, Visualization, Writing - original draft, Writing - review & editing. **Yonatan Loewenstein:** Conceptualization, Data curation, Formal analysis, Funding acquisition, Methodology, Project administration, Resources, Software, Supervision, Validation, Visualization, Writing - original draft, Writing - review & editing.

Acknowledgments

We thank N. Klein for critical assistant with figure graphicsWe are grateful to Tsahi Asher for fruitful discussions.We thank the ELSC MRI unit, Assaf Yohalashet, Lee Ashkenazi and Yuval Porat for their dedicated work.

Supplementary materials

Supplementary material associated with this article can be found, in the online version, at doi:10.1016/j.neuroimage.2020.117257.

References

Alain, C., Arnott, S.R., Hevenor, S., Graham, S., Grady, C.L., 2001. “What” and “where” in the human auditory system. Proc. Natl. Acad. Sci. U. S. A. 98, 12301–12306. doi:10.1073/pnas.211209098.

Amano, K., Wandell, B.A., Dumoulin, S.O., 2009. Visual field maps, population receptive field sizes, and visual field coverage in the human MT+ complex. J. Neurophysiol. 102, 2704–2718. doi:10.1152/jn.00102.2009.

Ann Stringer, E., Qiao, P.-G., Friedman, R.M., Holroyd, L., Newton, A.T., Gore, J.C., Min Chen, L., 2014. Distinct fine-scale fMRI activation patterns of contra- and ipsilateral somatosensory areas 3b and 1 in humans. Hum. Brain Mapp. 35, 4841–4857. doi:10.1002/hbm.22517.

Arienzo, D., Babiloni, C., Ferretti, A., Caulo, M., Del Gratta, C., Tartaro, A., Rossini, P.M., Romani, G.L., 2006. Somatotopy of anterior cingulate cortex (ACC) and supplementary motor area (SMA) for electric stimulation of the median and tibial nerves: an fMRI study. Neuroimage 33, 700–705. doi:10.1016/j.neuroimage.2006.06.030.

Arroyo, S., Lesser, R.P., Poon, W.-T., Robert, W., Webber, S., Gordon, B., 1997. Neuronal generators of visual evoked potentials in humans: visual processing in the human cortex. Epilepsia 38, 600–610. doi:10.1111/j.1528-1157.1997.tb01146.x.

Benjamini, Y., Hochberg, Y., 1995. Controlling the false discovery rate: a practical and powerful approach to multiple testing. J. R. Stat. Soc. Ser. B 57, 289–300. doi:10.1111/j.2517-6161.1995.tb02031.x.

Binkofski, F., Buxbaum, L.J., 2013. Two action systems in the human brain. Brain Lang. 127, 222–229. doi:10.1016/J.BANDL.2012.07.007.

Burkhalter, A., Van Essen, D.C., 1986. Processing of color, form and disparity information in visual areas VP and V2 of ventral extrastriate cortex in the macaque monkey. J. Neurosci. 6, 2327–2351. doi:10.1523/JNEUROSCI.06-08-02327.1986.

Culham, J., 1998. Timing in the visual hierarchy. Trends Cogn. Sci. 2, 473. doi:10.1016/S1364-6613(98)01264-9.

Deiber, M.P., Ibanez, V., Sadato, N., Hallett, M., 1996. Cerebral structures participating in motor preparation in humans: a positron emission tomography study. J. Neurophysiol. 75, 233–247. doi:10.1152/jn.1996.75.1.233.

Desikan, R.S., Ségonne, F., Fischlb, B., Quinn, B.T., Dickerson, B.C., Blacker, D., Buckner, R.L., Dale, A.M., Maguire, R.P., Hyman, B., Albert, M.S., Killiany, R.J., 2006. An automated labeling system for subdividing the human cerebral cortex on MRI scans into gyral based regions of interest. Neuroimage 31, 968–980. doi:10.1016/J.NEUROIMAGE.2006.01.021.

DeYoe, E.A., Van Essen, D.C., 1988. Concurrent processing streams in monkey visual cortex. Trends Neurosci. 11, 219–226. doi:10.1016/0166-2236(88)90130-0.

Dijkerman, H.C., de Haan, E.H.F., 2007. Somatosensory processing subserving perception and action: dissociations, interactions, and integration. Behav. Brain Sci. 30, 224–230. doi:10.1017/S0140525X07001641.

Duffy, F.H., Burchfiel, J.L., 1971. Somatosensory system: organizational hierarchy from single units in monkey area 5. Science 172, 273–275. doi:10.1126/science.172.3980.273.

Dumoulin, S.O., Wandell, B.A., 2008. Population receptive field estimates in human visual cortex. Neuroimage 39, 647–660. doi:10.1016/j.neuroimage.2007.09.034.

Eickhoff, S.B., Grefkes, C., Fink, G.R., Zilles, K., 2008. Functional lateralization of face, hand, and trunk representation in anatomically defined human somatosensory areas. Cereb. Cortex 18, 2820–2830. doi:10.1093/cercor/bhn039.

Felleman, D.J., Van Essen, D.C., 1991. Distributed hierarchical processing in the primate cerebral cortex. Cereb. Cortex 1, 1–47. doi:10.1093/cercor/1.1.1-a.

Friedman, D.P., Murray, E.A., O’Neill, J.B., Mishkin, M., 1986. Cortical connections of the somatosensory fields of the lateral sulcus of macaques: evidence for a corticolimbic pathway for touch. J. Comp. Neurol. 252, 323–347. doi:10.1002/cne.902520304.

Fuster, J.M., 1993. Frontal lobes. Curr. Opin. Neurobiol. 3, 160–165. doi:10.1016/0959-4388(93)90204-C.

Glasser, M.F., Coalson, T.S., Robinson, E.C., Hacker, C.D., Harwell, J., Yacoub, E., Ugurbil, K., Andersson, J., Beckmann, C.F., Jenkinson, M., Smith, S.M., Van Essen, D.C., 2016. A multi-modal parcellation of human cerebral cortex. Nature 536, 171–178. doi:10.1038/nature18933.

Goodale, M.A., Milner, A.D., 1992. Separate visual pathways for perception and action. Trends Neurosci. 15, 20–25. doi:10.1016/0166-2236(92)90344-8.

Graziano, M., 2006. The organization of behavioral repertoire in motor cortex. Annu. Rev. Neurosci. 29, 105–134. doi:10.1146/annurev.neuro.29.051605.112924.

Graziano, M.S.A., Yap, G.S., Gross, C.G., 1994. Coding of visual space by premotor neurons. Science 266, 1054–1057. doi:10.1126/science.7973661.

Grill-Spector, K., Malach, R., 2004. The human visual cortex. Annu. Rev. Neurosci. 27, 649–677. doi:10.1146/annurev.neuro.27.070203.144220.

Hagen, M.C., Zald, D.H., Thornton, T.A., Pardo, J.V., 2002. Somatosensory processing in the human inferior prefrontal cortex. J. Neurophysiol. 88, 1400–1406. doi:10.1152/jn.2002.88.3.1400.

Harvey, B.M., Klein, B.P., Petridou, N., Dumoulin, S.O., 2013. Topographic representation of numerosity in the human parietal cortex. Science 341, 1123–1126. doi:10.1126/science.1239052.

Hayashi, N., Nishijo, H., Ono, T., Endo, S., Tabuchi, E., 1995. Generators of somatosensory evoked potentials investigated by dipole tracing in the monkey. Neuroscience 68, 323–338. doi:10.1016/0306-4522(95)00126-4.

Huang, R.-S., Sereno, M.I., 2018. Multisensory and sensorimotor maps. Handb. Clin. Neurol. 151, 141–161. doi:10.1016/B978-0-444-63622-5.00007-3.

Hubel, D.H., Wiesel, T.N., 1962. Receptive fields, binocular interaction and functional architecture in the cat's visual cortex. J. Physiol. 160, 106–154. doi:10.1113/jphysiol.1962.sp006837.

Hyvärinen, J., Poranen, A., 1978. Receptive field integration and submodality convergence in the hand area of the post-central gyrus of the alert monkey. J. Physiol. 283, 539–556. doi:10.1113/jphysiol.1978.sp012518.

Inui, K., Wang, X., Tamura, Y., Kaneoke, Y., Kakigi, R., 2004. Serial processing in the human somatosensory system. Cereb. Cortex 14, 851–857. doi:10.1093/cercor/bhh043.

Iwamura, Y., 2003. Somatosensory association cortices. Int. Congr. Ser. 1250, 3–14. doi:10.1016/S0531-5131(03)00971-3.

Iwamura, Y., 1998. Hierarchical somatosensory processing. Curr. Opin. Neurobiol. 8, 522–528. doi:10.1016/S0959-4388(98)80041-X.

Iwamura, Y., Tanaka, M., Sakamoto, M., Hikosaka, O., 1993. Rostrocaudal gradients in the neuronal receptive field complexity in the finger region of the alert monkey's postcentral gyrus. Exp. Brain Res. 92, 360–368. doi:10.1007/BF00229023.

Kaas, J.H., 2004. Somatosensory system. The Human Nervous System. Paxinos G.

Kaas, J.H., Hackett, T.A., 1999. "What" and "where" processing in auditory cortex. Nat. Neurosci. 2, 1045–1047. doi:10.1038/15967.

Kaas, J.H., Nelson, R., Sur, M., Lin, C., Merzenich, M., 1979. Multiple representations of the body within the primary somatosensory cortex of primates. Science 204, 521–523. doi:10.1126/science.107591.

Kandel, E., Schwartz, J., Jessell, T., 2000. Principles of Neural Science. McGraw-Hill Medical.

Kastner, S., De Weerd, P., Pinsk, M.A., Elizondo, M.I., Desimone, R., Ungerleider, L.G., 2001. Modulation of sensory suppression: implications for receptive field sizes in the human visual cortex. J. Neurophysiol. 86, 1398–1411. doi:10.1152/jn.2001.86.3.1398.

Killackey, H.P., Gould, H.J., Cusick, C.G., Pons, T.P., Kaas, J.H., 1983. The relation of corpus callosum connections to architectonic fields and body surface maps in sensorimotor cortex of new and old world monkeys. J. Comp. Neurol. 219, 384–419. doi:10.1002/cne.902190403.

Kravitz, D.J., Saleem, K.S., Baker, C.I., Mishkin, M., 2011. A new neural framework for visuospatial processing. Nat. Rev. Neurosci. 12, 217–230. doi:10.1038/nrn3008.

Lee, K.M., Chang, K.H., Roh, J.K., 1999. Subregions within the supplementary motor area activated at different stages of movement preparation and execution. Neuroimage 9, 117–123. doi:10.1006/nimg.1998.0393.

Leinonen, L., Hyvarinen, J., Nyman, G., Linnankoski, I., 1979. I. Functional properties of neurons in lateral part of associative area 7 in awake monkeys. Exp. Brain Res. 34, 299–320. doi:10.1007/BF00235675.

Margulies, D.S., Ghosh, S.S., Goulas, A., Falkiewicz, M., Huntenburg, J.M., Langs, G., Bezgin, G., Eickhoff, S.B., Castellanos, F.X., Petrides, M., Jefferies, E., Smallwood, J., 2016. Situating the default-mode network along a principal gradient of macroscale cortical organization. Proc. Natl. Acad. Sci. U. S. A. 113, 12574–12579. doi:10.1073/pnas.1608282113.

Martin, A.B., Yang, X., Saalmann, Y.B., Wang, L., Shestyuk, A., Lin, J.J., Parvizi, J., Knight, R.T., Kastner, S., 2019. Temporal dynamics and response modulation across the human visual system in a spatial attention task: an ECoG study. J. Neurosci. 39, 333–352. doi:10.1523/JNEUROSCI.1889-18.2018.

Mazzola, L., Isnard, J., Mauguière, F., 2005. Somatosensory and pain responses to stimulation of the second somatosensory area (SII) in humans. A comparison with SI and insular responses. Cereb. Cortex 16, 960–968. doi:10.1093/cercor/bhj038.

Mesulam, M., 1998. From sensation to cognition. Brain 121, 1013–1052. doi:10.1093/brain/121.6.1013.

Milner, D., Goodale, M., 2006. The Visual Brain in Action. Oxford University Press doi:10.1093/acprof:oso/9780198524724.001.0001.

Mishkin, M., 1979. Analogous neural models for tactual and visual learning. Neuropsychologia 17, 139–151. doi:10.1016/0028-3932(79)90005-8.

Mitchell, J.S.B., Mount, D.M., Papadimitriou, C.H., 1987. Discrete geodesic problem. SIAM J. Comput. 16, 647–668. doi:10.1137/0216045.

Murata, A., Ishida, H., 2007. Representation of bodily self in the multimodal parieto-premotor network. In: Representation and Brain. Springer, Japan, pp. 151–176. doi:10.1007/978-4-431-73021-7_6.

Penfield, W., Boldrey, E., 1937. Somatic motor and sensory representation in the cerebral cortex of man as studied by electrical stimulation. Brain 60, 389–443. doi:10.1093/brain/60.4.389.

Penfield, W., Jasper, H., 1954. Epilepsy and the Functional Anatomy of the Human Brain. Little, Brown & Co., Oxford.

Penfield, W., Rasmussen, T., 1950. The Cerebral Cortex of Man; A Clinical Study of Localization of Function. Hafner, New York.

Pigarev, I.N., Nothdurft, H.-C., Kastner, S., 2001. Neurons with large bilateral receptive fields in monkey prelunate gyrus. Exp. Brain Res. 136, 108–113. doi:10.1007/s002210000566.

Power, J.D., Cohen, A.L., Nelson, S.M., Wig, G.S., Barnes, K.A., Church, J.A., Vogel, A.C., Laumann, T.O., Miezin, F.M., Schlaggar, B.L., Petersen, S.E., 2011. Functional network organization of the human brain. Neuron 72, 665–678. doi:10.1016/j.neuron.2011.09.006.

Puckett, A.M., Bollmann, S., Junday, K., Barth, M., Cunnington, R., 2020. Bayesian population receptive field modeling in human somatosensory cortex. Neuroimage 208, 116465. doi:10.1016/j.neuroimage.2019.116465.

Reed, C.L., Hagler, D.J., Marinkovic, K., Dale, A., Halgren, E., 2009. Sequences of cortical activation for tactile pattern discrimination using magnetoencephalography. Neuroreport 20, 941–945. doi:10.1097/WNR.0b013e32832c5f65.

Reed, C.L., Klatzky, R.L., Halgren, E., 2005. What vs. where in touch: an fMRI study. Neuroimage 25, 718–726. doi:10.1016/j.neuroimage.2004.11.044.

Rizzolatti, G., Fogassi, L., Gallese, V., 2002. Motor and cognitive functions of the ventral premotor cortex. Curr. Opin. Neurobiol. 12, 149–154. doi:10.1016/S0959-4388(02)00308-2.

Robinson, C.J., Burton, H., 1980. Organization of somatosensory receptive fields in cortical areas 7b, retroinsula, postauditory and granular insula ofM. fascicularis. J. Comp. Neurol. 192, 69–92. doi:10.1002/cne.901920105.

Rolanc, P.E., Zilles, K., 1996. Functions and structures of the motor cortices in humans. Curr. Opin. Neurobiol. 6, 773–781. doi:10.1016/S0959-4388(96)80027-4.

Romanski, L.M., Tian, B., Fritz, J., Mishkin, M., Goldman-Rakic, P.S., Rauschecker, J.P., 1999. Dual streams of auditory afferents target multiple domains in the primate prefrontal cortex. Nat. Neurosci. 2, 1131–1136. doi:10.1038/16056.

Rousselet, G.A., Thorpe, S.J., Fabre-Thorpe, M., 2004. How parallel is visual processing in the ventral pathway? Trends Cogn. Sci. 8, 363–370. doi:10.1016/J.TICS.2004.06.003.

Ruben, J., Schwiemann, J., Deuchert, M., Meyer, R., Krause, T., Curio, G., Villringer, K., Kurth, R., Villringer, A., 2001. Somatotopic organization of human secondary somatosensory cortex. Cereb. Cortex 11, 463–473. doi:10.1093/cercor/11.5.463.

Saadon-Grosman, N., Loewenstein, Y., Arzy, S., 2020. The 'creatures' of the human cortical somatosensory system. Brain Commun. 2. doi:10.1093/BRAINCOMMS/FCAA003.

Saadon-Grosman, N., Tal, Z., Itshayek, E., Amedi, A., Arzy, S., 2015. Discontinuity of cortical gradients reflects sensory impairment. Proc. Natl. Acad. Sci. U. S. A. 112, 16024–16029. doi:10.1073/pnas.1506214112.

Sakata, H., Takaoka, Y., Kawarasaki, A., Shibutani, H., 1973. Somatosensory properties of neurons in the superior parietal cortex (area 5) of the rhesus monkey. Brain Res. 64, 85–102. doi:10.1016/0006-8993(73)90172-8.

Schellekens, W., Petridou, N., Ramsey, N.F., 2018. Detailed somatotopy in primary motor and somatosensory cortex revealed by Gaussian population receptive fields. Neuroimage 179, 337–347. doi:10.1016/j.neuroimage.2018.06.062.

Schmolesky, M.T., Wang, Y., Hanes, D.P., Thompson, K.G., Leutgeb, S., Schall, J.D., Leventhal, A.G., 1998. Signal timing across the macaque visual system. J. Neurophysiol. 79, 3272–3278. doi:10.1152/jn.1998.79.6.3272.

Schwoebel, J., Coslett, H.B., 2005. Evidence for multiple, distinct representations of the human body. J. Cogn. Neurosci. 17, 543–553. doi:10.1162/0898929053467587.

Sereno, M.I., Huang, R.-S., 2014. Multisensory maps in parietal cortex. Curr. Opin. Neurobiol. 24, 39–46. doi:10.1016/J.CONB.2013.08.014.

Sereno, M.I., Huang, R.S., 2006. A human parietal face area contains aligned head-centered visual and tactile maps. Nat. Neurosci. 9, 1337–1343. doi:10.1038/nn1777.

Takaura, K., Tsuchiya, N., Fujii, N., 2016. Frequency-dependent spatiotemporal profiles of visual responses recorded with subdural ECoG electrodes in awake monkeys: differences between high- and low-frequency activity. Neuroimage 124, 557–572. doi:10.1016/j.neuroimage.2015.09.007.

Tal, Z., Geva, R., Amedi, A., 2016. The origins of metamodality in visual object area LO: bodily topographical biases and increased functional connectivity to S1. Neuroimage 127, 363–375. doi:10.1016/J.NEUROIMAGE.2015.11.058.

Taoka, M., Toda, T., Iwamura, Y., 1998. Representation of the midline trunk, bilateral arms, and shoulders in the monkey postcentral somatosensory cortex. Exp. Brain Res. 123, 315–322. doi:10.1007/s002210050574.

Van Boven, R.W., Ingeholm, J.E., Beauchamp, M.S., Bikle, P.C., Ungerleider, L.G., 2005. Tactile form and location processing in the human brain. Proc. Natl. Acad. Sci. U. S. A. 102, 12601–12605. doi:10.1073/pnas.0505907102.

Ungerleider, L.G., Mishkin, M., 1982. Two cortical visual systems. In: Analysis of Visible Behaviour. MIT Press, Cambridge, pp. 549–586.

Wandell, B.A., Dumoulin, S.O., Brewer, A.A., 2007. Visual field maps in human cortex. Neuron 56, 366–383. doi:10.1016/J.NEURON.2007.10.012.

Wandell, B.A., Winawer, J., 2011. Imaging retinotopic maps in the human brain. Vis. Res. 51, 718–737. doi:10.1016/j.visres.2010.08.004.

Yoshor, D., Bosking, W.H., Ghose, G.M., Maunsell, J.H.R., 2007. Receptive fields in human visual cortex mapped with surface electrodes. Cereb. Cortex 17, 2293–2302. doi:10.1093/cercor/bhl138.

Young, J.P., Herath, P., Eickhoff, S., Choi, J., Grefkes, C., Zilles, K., Roland, P.E., 2004. Somatotopy and attentional modulation of the human parietal and opercular regions. J. Neurosci. 24, 5391–5399. doi:10.1523/JNEUROSCI.4030-03.2004.